

# Laser texturing of piston ring for tribological performance improvement

Rita FERREIRA<sup>1,2,3,4,\*</sup>, Óscar CARVALHO<sup>1,2</sup>, Luís SOBRAL<sup>4</sup>, Sandra CARVALHO<sup>3</sup>, Filipe SILVA<sup>1,2</sup>

<sup>1</sup> CMEMS–UMinho, University of Minho, Guimarães 4800058, Portugal

<sup>2</sup> LABBELS–Associate Laboratory, Guimarães 4800058, Portugal

<sup>3</sup> CEMMPRE–Center for Mechanical Engineering, Materials and Processes, University of Coimbra, Rua Luís Reis Santos, Coimbra 3030-788, Portugal

<sup>4</sup> MAHLE, Componentes de Motores, S.A., Núcleo Industrial de Murte de, Cantanhede 3060-372, Portugal

Received: 20 June 2022 / Revised: 21 September 2022 / Accepted: 09 November 2022

© The author(s) 2022.

**Abstract:** The radial surface coating layer of compression piston rings is used to improve their wear resistance during the internal combustion engine operation. However, at top dead centers, the friction coefficient of the piston ring–cylinder liner pair is detrimental to the engine’s tribological performance. In this work, dimples with different texture dimensions and densities were tested in a home-developed tribometer. The friction coefficient was measured for all samples, and for those with the best results, their wear resistance was assessed. The texture with an aspect ratio of 0.25 and a density area of 15% reported the best tribological results.

**Keywords:** piston ring; surface texture; friction; wear

## 1 Introduction

A reciprocating sliding movement between the engine piston and its respective cylinder liner occurs during internal combustion engine operation. Assembled to the piston, the compression piston ring acts as a combustion chamber sealing with a continuous contact against the inner liner. The piston assembly, where the piston ring–cylinder contact, represents most of the internal combustion engine frictional losses, between 45% and 55% [1].

Lubricating oils minimize those mechanical losses and the consequent influence on the vehicle’s performance [2]. However, the presence and the characteristics of a lubricant layer between the piston ring radial surface and the inner cylinder surface depend on the current engine stroke [3, 4]. Distinct lubricant regimes occur during the four strokes, from starved to boundary and hydrodynamic. Top dead-centers, particularly the combustion stroke, gather the most detrimental conditions for the compression

piston ring: the maximum gas temperature, the maximum gas pressure, and an almost null sliding speed. As a result, severe scuffing wear of the compression piston ring results in significant frictional losses associated with this tribological pair.

Engineered and textured surfaces developed with a functional purpose are already recognized as available methods to confer desirable surface properties through a specific pattern topography [5, 6]. In the compression piston ring component, the characteristics of its radial surface have a determinant influence on the piston ring–cylinder liner contact [7]. For a tribological purpose, the laser surface treatment of the top ring radial surface has been extensively studied in the academic literatures through experimental [8, 9] and numerical studies [10–13].

Laser surface texturing represents a potential tool for friction reduction applications with feasible implementation in large-scale production. If properly distributed, the resultant surface textures will allow the entrapment of wear debris in the texture pockets

\* Corresponding author: Rita FERREIRA, E-mail: rita.mac.ferreira@gmail.com

and act as secondary lubricant reservoirs. On the surface of the piston ring, surface texturing may represent a way to avoid scuffing/spalling issues.

The main functional arguments used for surface texture implementation are the lubricant supply in cases of starved lubrication (acting as micro-reservoirs) and the effect of micro-hydrodynamic bearings during a hydrodynamic lubrication regime, and the entrapment of wear debris.

In cooperation with different researchers, Etsion [8, 14–19] produced several studies embracing laser surface texturing and their application in the piston ring–cylinder liner tribological pair. The use of partial texturing, instead of a total textured surface area, is suggested by Etsion's research group for parallel and flat surfaces, such as the contact of mechanical seals [18, 19]. Etsion and Sher [8] investigated the influence of partial laser surface texturing of the top piston rings on fuel consumption and reduced it up to 4%.

Lu and Wood [20] published a review paper focused on the surface texturing process applied to mechanical systems. One of their conclusions was the detrimental effect of deep dimples, and that optimal depth value is dependent on the working conditions. Braun et al. [21] studied the efficiency of laser surface texturing in reducing friction under mixed lubrication. They concluded that an optimum texture is found only for specific operation conditions, even considering the oil temperature and oil viscosity.

One of the most common conclusions found in the published research papers is the reliance on surface texturing effectiveness on several intrinsic and extrinsic parameters. The type of contact, functional conditions, texture dimensions, and geometries represent determinant variables [22–24], together with the component's material and the lubricating oil properties.

Although textures in the piston ring's surface do not yet represent a commercial solution, the surface texturing of the cylinder liner bore is already implemented. Cross-hatched geometries are produced into the cylinder bore to create a plateau-honing surface finishing to foster oil circulation [25–28]. Even in the cylinder liner, the surface texturing is performed where the piston inverts its sliding movement, which is associated with an increase in friction coefficient.

Grabon et al. [27, 29] studied the tribological response of the honing texture and, more specifically, the honing angles in the cylinder liner's inner surface.

Rao et al. [30] studied the effect of simultaneous surface texture in a diesel engine's cylinder liner inner surface and piston ring radial surface. They used different groove widths in the cylinder liner surface and dimples of 1 mm in the piston ring surface. In conclusion, the cylinder liner with a larger groove texture (3 mm) associated with a non-textured piston ring can reduce exhaust gas emissions. Miao et al. [31] also evaluated the tribological behavior of the co-textured cylinder liner-piston ring during the running-in of a marine diesel engine. Dimple textures on the piston ring surface are more effective as a mobile oil reservoir than the groove texture on the cylinder liner.

Several authors investigate the combination of surface texturing and thin coating films. Some published studies performed a preliminary surface texturing of the substrate [32–34]. Other works produced micropatterns in the coating layer with a tribological purpose [24, 35]. Sedlaček et al. [24] confirmed the beneficial effect of combining coating deposition and texturing (according to this sequence) to decrease the friction coefficient further.

In the present study, a laser surface treatment is applied to a commercial compression piston ring used in heavy-duty diesel engines to produce micro dimples along the radial ring surface. The piston ring possesses an NbN/CrN coating layer, which is used to improve its wear resistance. The influence of the micro dimples in the piston ring tribological response is evaluated using a home-developed tribometer. The coefficient of friction and the wear mass loss of textured and untextured samples were analyzed and compared.

## 2 Experimental procedure

### 2.1 Piston ring characterization

The compression piston rings have an NbN/CrN layer deposited by an industrial cathodic arc plasma equipment. The coatings were produced from pure chromium and niobium targets and a nitrogen atmosphere. The substrate was gas nitrided martensitic

stainless steel piston rings [36]. A Cr bonding layer was deposited to improve the adhesion between the stainless steel substrate and the deposited coating.

Before the surface texturing treatment, the piston ring and the coating layer were characterized. The surface and cross-sectional analysis of the coatings' morphology was performed by scanning electron microscopy (SEM) (JSM-6010 LV, JEOL). The thickness of the layers was obtained through a cross-sectional study also by SEM. The in-depth chemical composition measurements were performed throughout its profile, using SEM and the connected energy dispersive spectroscopy (EDS) (INCAx-Act, PentaFET Precision, Oxford Instruments) equipment. Additional qualitative and semi-quantitative chemical composition assessments were performed using the same equipment.

The resultant piston ring surface textures were also dimensionally characterized using the SEM micrographs and an image processing software (ImageJ).

The analysis by X-ray diffraction (XRD) (Bruker D8 Discover) was selected to study the coating's internal crystalline structure. This analysis comprised a classical  $\theta$ - $2\theta$  diffractometer with a Bragg–Brentano geometry using  $\text{CuK}\alpha$  radiation. The step size was  $0.04^\circ 2\theta$ , with 4 s/step and a  $2\theta$  range of  $15^\circ$ – $90^\circ$ .

Hardness measurements were performed using a Micro Materials NanoTest indentation system with 750 mN. The hardness value represents the average of at least ten measurements. To minimize the substrate influence, the indentation depths were up to 10% of the coating thickness. These measurements also allowed us to determine Young's modulus.

## 2.2 Surface texturing process

The functional surface of commercial compression piston rings was modified for the present study. The round dimples were produced using a microsecond pulsed laser (Model: XM-30D Fiber Laser Marking Machine) with a wavelength of 1,064 nm and a maximum power of 30 W (frequency up to 100 kHz). The spacing between the micro dimple patterns varies according to the laser frequency. In the present work, the laser beam scanning speed was moved with a velocity ranging from 7,500 to 15,000 mm/s.

After surface texturing, the piston rings underwent an additional lapping stage. The post-texturing lapping

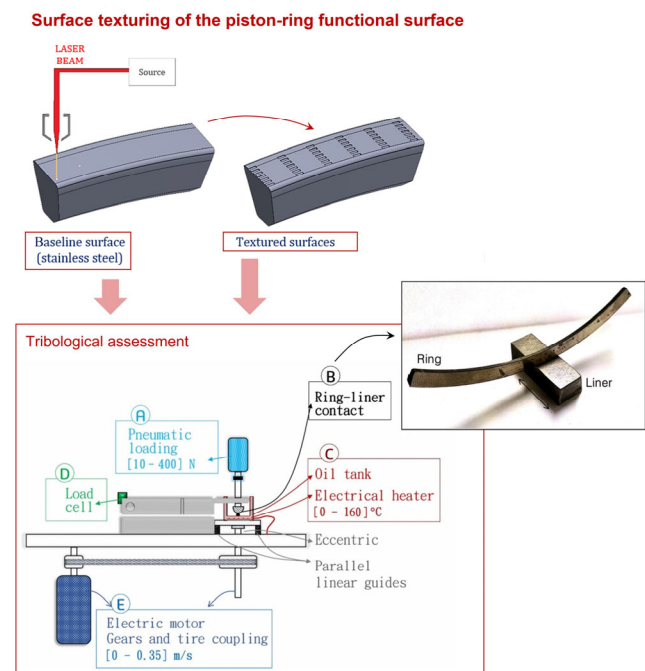
is a determinant of removing possible remelting material and consequent bulges around the rim and controlling the coating's surface roughness.

## 2.3 Testing method and test conditions

The present work uses a home-developed tribometer designed to fit standard ring–liner pair of heavy-duty diesel engines [37]. The baseline and textured ring samples were tested against cast iron cylinder liner pieces. A schematic view of the test rig is presented in Fig. 1.

The rig consists of five subsystems identified in Fig. 1 from A to E. The sliding contact had 10 mm of stroke. The liner samples have the typical plateau-honed surface texture existing in the cylinder bore.

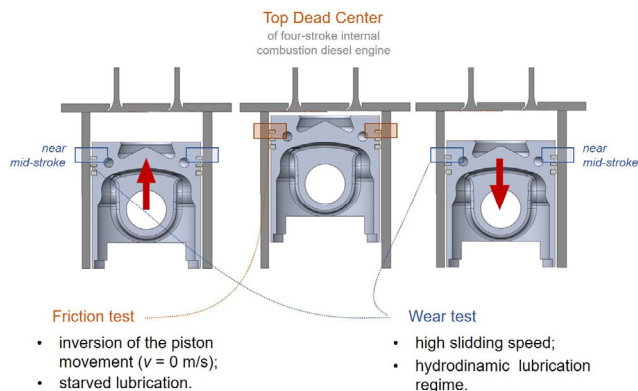
The coefficient of friction and wear resistance were analyzed according to different parameters, exhibited in Table 1. Based on the four-stroke diesel engine, the frictional response was evaluated by reproducing the top dead center conditions, as indicated in Fig. 2. With the piston's inversion of movement, the sliding speed decreases to zero, and the effect of the radial force reduces the oil film, creating a starved lubrication condition. The lubrication regime was created using a syringe with a 0.0258 ml of oil dosage dispensed



**Fig. 1** Schematic representation of the home-developed test rig used to evaluate the tribological response of the piston ring–cylinder liner tribological pair.

**Table 1** Specific friction and wear testing conditions used in the tribological assessment.

Parameter	Friction test	Wear test
Sliding speed	0.026 m/s	0.3 m/s
Normal load	10–11 N	350–380 N
Lubricating oil	0W20	0W20
Lubrication	Boundary regime	Fully flooded regime flooded
Oil temperature	20 ± 3 °C	135 ± 5 °C
Oil contaminant	—	Al <sub>2</sub> O <sub>3</sub> (5 μm)

**Fig. 2** Friction and wear test approach.

into the contacting area. The association of the lower sliding speed and the boundary lubrication regime reproduced a starved lubrication condition, characteristic of top dead center (TDC) stroke. The coefficient of friction and the sliding time were continuously recorded.

The wear test protocol reproduced the overall performance of the piston ring during the four-stroke cycle. The high sliding speed achieved by the piston near the mid-stroke into the liner is associated with the hydrodynamic lubrication regime. To foster the ring and liner surface's wear and consequently allow the quantification of their mass loss, 3.5 g of alumina particles were dispersed per 700 mL of lubrication oil. An oil contaminant is widespread in industrial protocols. Otherwise, substantially longer tests would be demanded to observe worn surfaces.

Before the sample's analysis, a cleaning operation is used to remove the lubrication oil and wear debris from the sliding contact. The sample mass was measured before and after the tribological assessment using an analytical balance Kern ABS-N/ABJ-NM with 0.0001 g accuracy. The worn surface morphology of the piston ring and the cylinder liner was characterized through SEM and EDS techniques.

### 3 Results and discussion

#### 3.1 Morphological, crystallographic, and mechanical characterization

The transition metal nitride coating deposited on the SS substrate and the respective Cr interlayer are exhibited in Fig. 3. The CrN/NbN layer varies from 24 and 28 μm in thickness and presents a dense columnar microstructure. The chromium bonding layer possesses an average thickness of 1 μm and a columnar structure.

Figure 4 displays the in-depth chemical composition of the coating layer. The cross-sectional study of the fractured samples detected the presence of C, with a periodic increase in its content. At the end of the Cr bonding layer, Fe and C elements substantially increased because of the stainless steel chemical composition.

The phase composition of the coatings was characterized by observing the diffraction peaks in the range of 15°–90° using XRD. Figure 5 shows the  $\theta$ -2 $\theta$  XRD.

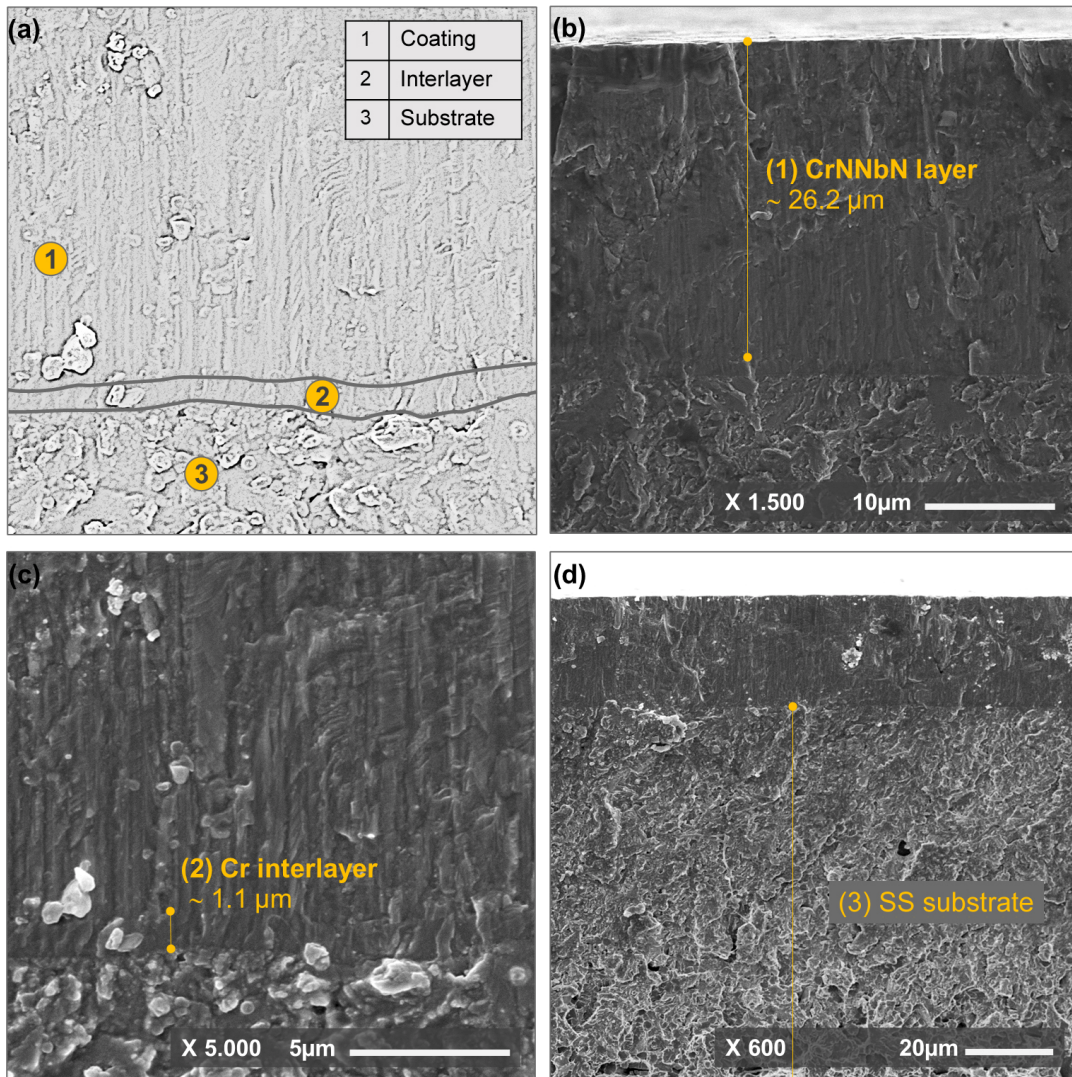
A broader range analysis, between 30° and 70°, identified two distinct peak concentration ranges. The most intense peaks related to NbN and CrN, ICDD #38-1155 and ICDD #11-65 cards, are in the magnified graph ( $2\theta$ : 32.5°–45°). The coating's mechanical properties were obtained through nanoindentation measurements. The mean hardness value resultant from ten measurements was 24.5 GPa (with a standard deviation of 3.02 GPa). The Young modulus value was 364 GPa, achieving a maximum indentation depth of around 1.4 μm.

#### 3.2 Characterization of surface textures

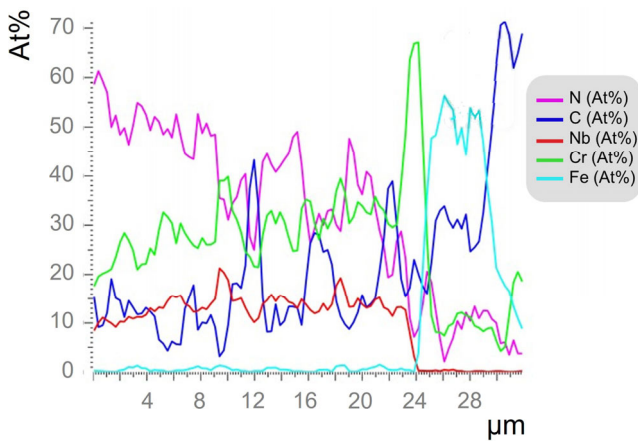
Different dimensional characteristics resulted from the laser power and laser scanning speed variation. Table 2 presents the dimensional characterization of the textured dimples using 15 W of laser power, constituting group 1 (G1), and 30 W, of group 2 (G2), and different laser speeds. Dimple's aspect ratio was defined as the ratio of the micro-dimple depth to the micro-dimple diameter. The density area represents the ratio of the micro-dimple area over a micro-dimple array. The surface dimples prepared in the present study are exhibited in Fig. 6.



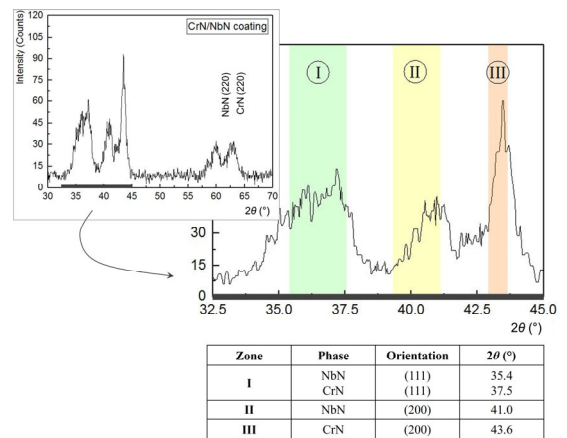
Figures were enumerated by (a), (b), (c) and (d) and the respective legend of each is below



**Fig. 3** SEM analysis of the piston ring cross-section with (a) a schematic representation of the piston ring’s layers and the detailed micrographs of (b) CrN/NbN coating, (c) Cr interlayer, and (d) SS substrate.



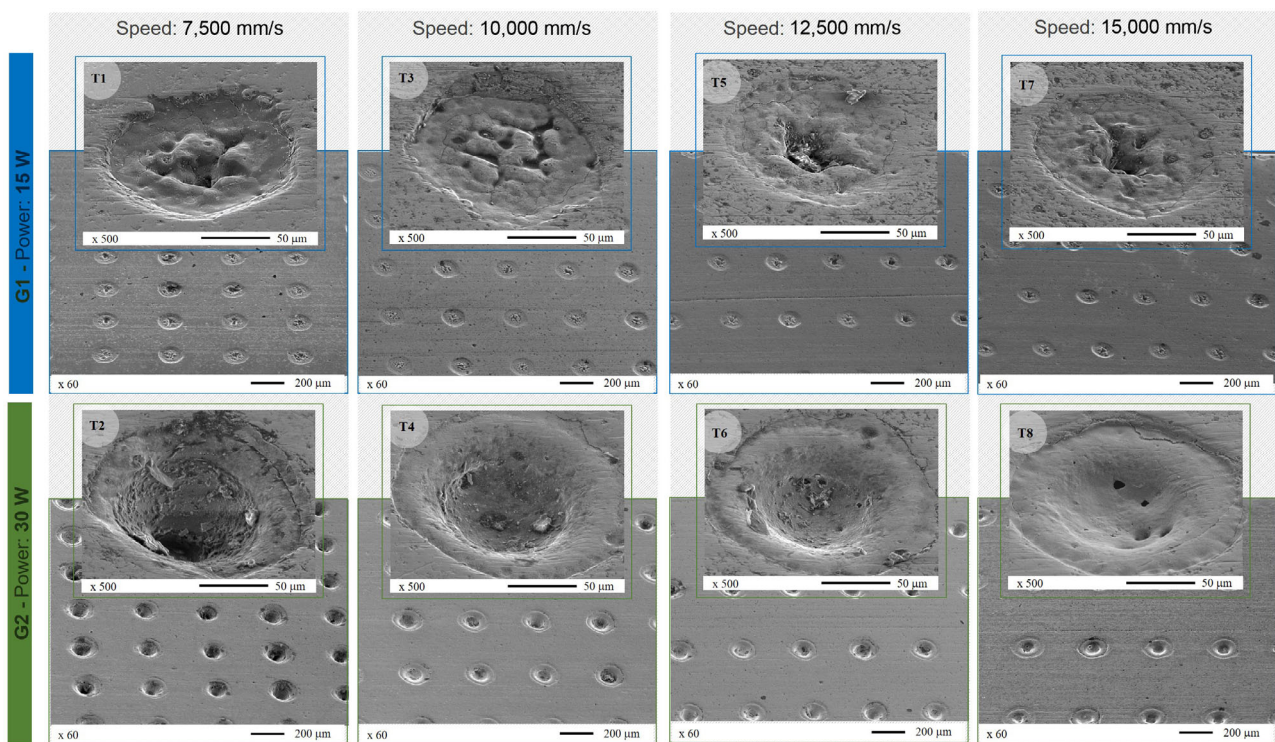
**Fig. 4** In-depth chemical composition of the CrN/NbN coating layer quantified by SEM-EDS.



**Fig. 5** XRD patterns for CrN/NbN coating layer with three peak zones (I, II, and III).

**Table 2** Dimensional characterization of piston ring dimples produced by laser surface texturing.

	Laser speed (mm/s)	Dimples dimensional characterization				
		$\varnothing_{\text{aver}}$ ( $\mu\text{m}$ )	Depth ( $\mu\text{m}$ )	Aspect ratio, $\lambda$	Pitch ( $\mu\text{m}$ )	Density area
G1		Power: 15 W				
T1	7,500	132	21	0.16	205	22%
T3	10,000	136	19	0.14	295	14%
T5	12,500	131	16	0.12	385	11%
T7	15,000	128	13	0.10	440	9%
G2		Power: 30 W				
T2	7,500	157	94	0.60	190	35%
T4	10,000	170	77	0.45	280	27%
T6	12,500	159	55	0.35	350	17%
T8	15,000	158	40	0.25	450	15%

**Fig. 6** SEM micrography of piston ring dimples produced by laser surface texturing.

The textures obtained using the lower laser power value present nearly the same dimple's diameter, around 130  $\mu\text{m}$ . The variation of the laser speed influenced the dimple's density area. A higher laser texturing speed resulted in spaced laser spots and, thus, an increased distance between consecutive dimples along the machining axis. The dimple's depth range between 13  $\mu\text{m}$  (T7) and 21  $\mu\text{m}$  (T1), with an aspect ratio of 0.1 and 0.16, respectively. The dimple's pitch

in the piston ring radial direction was constant for each group: 300  $\mu\text{m}$  for G1 and 280  $\mu\text{m}$  for G2. In the perpendicular direction, the dimple's pitch increased and, consequently, the density area decreased.

The increase of power (for 30W) fostered a higher laser energy density of the laser beam discharge. Deeper dimples and larger diameters lead to higher aspect ratio values and increase the obtained density area for the same laser speed.



### 3.3 Tribological results

The friction coefficient testing parameters replicate the most unfavorable conditions, similar to those during start-up under starved and mixed lubrication. Coefficient of friction (COF) values were recorded continuously during 5,000 cycles, and the average COF results (after the running in period) of non-texture and textured samples are exhibited in Fig. 7 for different time frames.

The baseline value was considered for the non-textured piston ring. T3, T4, and T5 textures revealed higher COF than non-textured samples during the entire trial. T2 and T6 textures presented a behavior similar to the baseline piston ring without significantly improving the frictional response. T1 and T8 improved the frictional performance, with a COF reduction of 14% and 4%, respectively, when compared with the non-textured surface. T7 evidenced an oscillatory

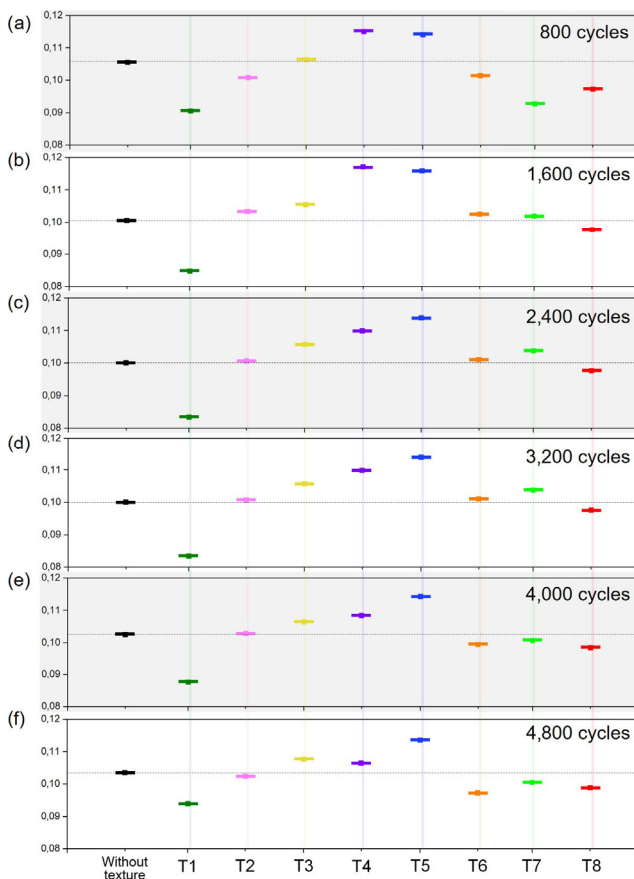


**Fig. 7** Average COF values of the non-textured and textured samples registered over six distinct time frames: (a) 800 cycles; (b) 1,600 cycles; (c) 2,400 cycles; (d) 3,200 cycles; (e) 4,000 cycles; and (f) 4,800 cycles.

response through the experiment, with a higher COF value up to 3,200 cycles, followed by a substantial reduction. The average result revealed a COF decrease of 2% for T7 texture.

Gachot et al. [38] presented a summary of surface texturing parameters depending on texture geometry and lubrication conditions. They concluded that a circular pocket is an effective texture geometry for diverse lubrication. Yet, the texture dimensions influence the entire tribological performance. In the absence of a clear trend of the texture's frictional behavior neither for G1 nor for G2, dimensional parameters presented in Table 2 were correlated with the tribological results. Figure 8 shows the average COF against dimple's density area, average diameter, and aspect ratio.

A minor variation in the average dimple's diameter of samples from both G1 and G2, of 132 and 161  $\mu\text{m}$ . Wu et al. [6] studied the influence of the surface texture parameters under starved lubrication. According to the simulation using TDC conditions, they concluded that distribution density was the parameter with a more significant influence on the COF reduction. The dimple's depth was the second most influential parameter, and the dimple's diameter influence was minor.

The best results were obtained for samples with a texture density of 0.15 and 0.22, and an aspect ratio in the range 0.16–0.28. Zavos and Nikolakopoulos [39] referenced similar values for an optimum aspect ratio. However, using either a different lubrication regime or the texturing of different contact geometries will define new optimum geometric and dimensional parameters. Schubert et al. [40] tested micro dimples on a flat ring-on-disc test rig under a fully-flooded regime and indicated 10% for the pattern density with the best friction coefficient. Wos et al. [41] evaluated the frictional response of dimpled textures, and those with 17% of area density achieved the best results under various lubrication regimes.

Those textures with the best COF results, T1 and T8, were submitted to a wear test to compare their wear resistance and effect on the cylinder liner counterpart with the non-textured samples. Figure 9 are samples' COF and the weight loss, either of the piston ring samples or the cylinder liner counterpart.

Piston rings already had the previously deposited

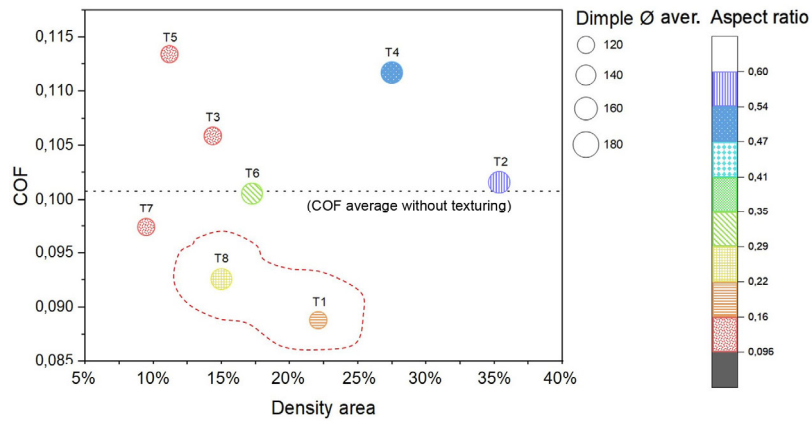


Fig. 8 Effect of texture’s geometric parameters on the COF results.

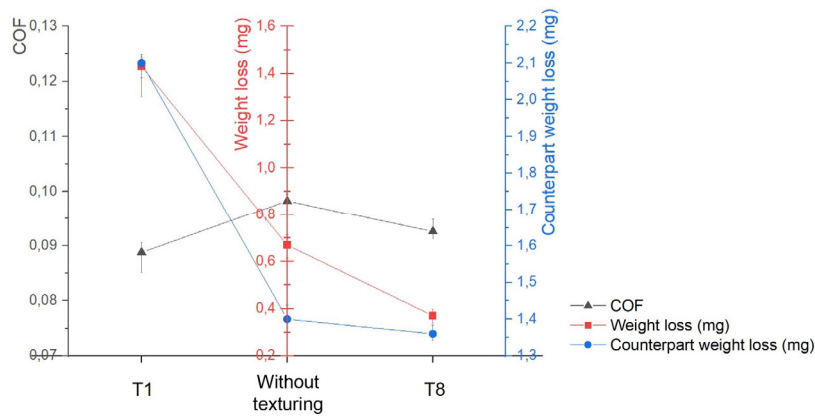


Fig. 9 Wear test results comprising piston ring and cylinder liner weight loss.

coating layer to improve their wear resistance. However, surface textures were expected to have an essential role in surface wear resistance. Arslan et al. [23] studied the tribological performance of a

pre-textured surface with subsequent deposition of a diamond-like carbon coating. The group with 20% area density got the best COF results and a lower wear rate than the untextured sample. Figure 10 exhibits the

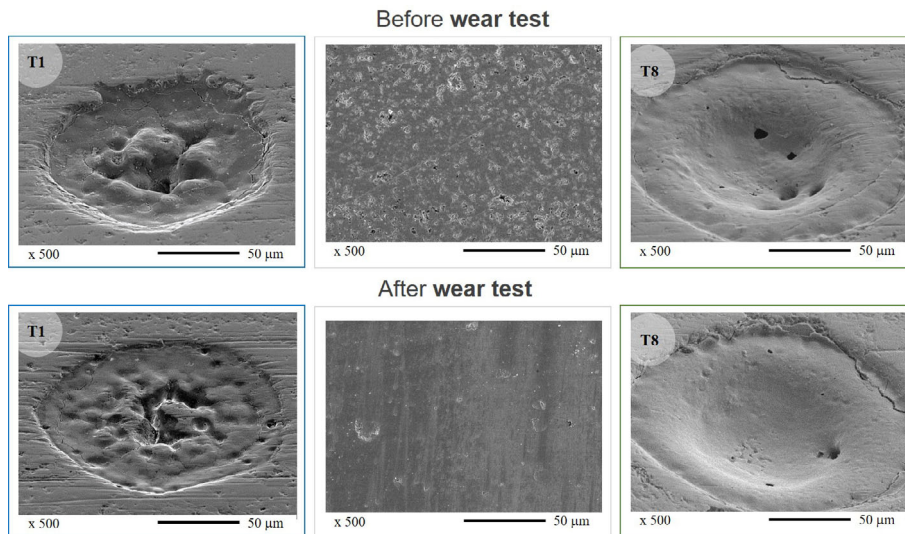


Fig. 10 SEM micrography of non-textured samples and T1 and T8 piston ring dimples before and after wear tests.



SEM images of the sample without texture and the T1 and T8 textures, before and after wear tests.

T1 was the texture with higher COF reduction but the worst performance in the wear test. The piston ring weight loss was superior to the untextured ring, and it produced an increased weight loss on the counterpart. After the wear test assessment, the entrapment of abrasive particles was noticed within some micro dimples. The shallower texture, T1, offered a lower volume for oil reservoirs and wear debris entrapment.

Conversely, deeper dimples of T8 created hydrodynamic pressure pockets. Under high sliding speed, the lubricant film thickness increased, and the contact occurred in a full fluid film lubricant regime.

The internal combustion engine operates in a complete duty cycle in different frictional regimes. T8 possessed the optimized dimple texture parameters, with a simultaneous improvement of the COF under a boundary lubrication regime and an enhanced wear resistance under a fully flooded film.

#### 4 Concluding remarks

Friction and wear have a significant influence on the engine's energy consumption. NbN/CrN coated piston rings used in heavy-duty diesel engines were textured and tribologically evaluated using a home-developed tribometer. Several texture dimensions and densities were tested in the compression ring functional surface. According to specified and optimized texturing parameters, micro dimples have the potential to reduce friction-induced wear.

The reported friction coefficient results show that aspect ratio and density area were decisive variables. The wear resistance of textured samples with an enhanced friction coefficient was also compared with the untextured piston ring. T8 presented an overall improvement in the tribological performance with a lower weight loss and a minimized effect on the cylinder liner surface simultaneously. The alternative to a single texture with a global optimized performance could be to apply different textures for distinct purposes.

Further studies are expected about the influence of the secondary movement of the piston ring into the ring groove on the optimum texture parameters.

#### Acknowledgements

This work was supported by Fundação para a Ciência e Tecnologia (FCT) and MAHLE, Componentes de Motores, S.A. through the grant SFRH/BDE/110654/2015 and by the project Add-Additive with the reference POCI-01-0247-FEDER- 024533.

#### Declaration of competing interest

The author has no competing interests to declare that are relevant to the content of this article.

**Open Access** This article is licensed under a Creative Commons Attribution 4.0 International License, which permits use, sharing, adaptation, distribution and reproduction in any medium or format, as long as you give appropriate credit to the original author(s) and the source, provide a link to the Creative Commons licence, and indicate if changes were made.

The images or other third party material in this article are included in the article's Creative Commons licence, unless indicated otherwise in a credit line to the material. If material is not included in the article's Creative Commons licence and your intended use is not permitted by statutory regulation or exceeds the permitted use, you will need to obtain permission directly from the copyright holder.

To view a copy of this licence, visit <http://creativecommons.org/licenses/by/4.0/>.

#### References

- [1] Holmberg K, Andersson P, Nylund NO, Mäkelä K, Erdemir A. Global energy consumption due to friction in trucks and buses. *Tribol Int* **78**: 94–114 (2014)
- [2] Tamura K, Kasai M. Impact of boundary lubrication performance of engine oils on friction at piston ring-cylinder liner interface yukinobu nakamura and tomoyuki enomoto. *Int J Fuels Lubr* **7**(3): 875–881 (2014)
- [3] Oliva A, Held S. Numerical multiphase simulation and validation of the flow in the piston ring pack of an internal combustion engine. *Tribol Int* **101**: 98–109 (2016)
- [4] Fatjo G G, Smith E H. Piston-ring film thickness: Theory and experiment compared. *Proc Inst Mech Eng Part J J Eng Tribol* **232**(5): 1–18 (2017)
- [5] Costa H L, Hutchings I M. Some innovative surface

- texturing techniques for tribological purposes. *Proc Inst Mech Eng Part J J Eng Tribol* **229**: 429–448 (2015)
- [6] Wu S, Zhang P, Wei H, Chen L. Influence of surface texture parameters on friction characteristics under starved lubrication. *Polish Marit Res* **27**: 96–106 (2020)
- [7] Ferreira R, Martins J, Carvalho Ó, Sobral L, Carvalho S, Silva F. Tribological solutions for engine piston ring surfaces: an overview on the materials and manufacturing. *Mater Manuf Process* **35**(5): 498–520 (2020)
- [8] Etsion I, Sher E. Improving fuel efficiency with laser surface textured piston rings. *Tribol Int* **42**: 542–547 (2009)
- [9] Shen C, Khonsari M M. The effect of laser machined pockets on the lubrication of piston ring prototypes. *Tribol Int* **101**: 273–283 (2016)
- [10] Dobrica M B, Fillon M, Pascovici M D, Cicone T. Optimizing surface texture for hydrodynamic lubricated contacts using a mass-conserving numerical approach. *Proc Inst Mech Eng Part J J Eng Tribol* **224**: 737–750 (2010)
- [11] Tomanik E. Modelling the hydrodynamic support of cylinder bore and piston rings with laser textured surfaces. *Tribol Int* **59**: 90–96 (2013)
- [12] Usman A, Park C W. Optimizing the tribological performance of textured piston ring-liner contact for reduced frictional losses in SI engine: Warm operating conditions. *Tribol Int* **99**: 224–236 (2016)
- [13] Gu C, Meng X, Xie Y, Yang Y. Effects of surface texturing on ring/liner friction under starved lubrication. *Tribol Int* **94**: 591–605 (2016)
- [14] Ronen A, Etsion I, Kligerman Y. Friction-reducing surface-texturing in reciprocating automotive components. *Tribol Trans* **44**: 359–366 (2001)
- [15] Ronen A, Kligerman Y, Etsion I. Different approaches for analysis of friction in surface textured reciprocating components. *Proc 2nd World* **2**: 2–5 (2001)
- [16] Etsion I. State of the art in laser surface texturing. *J Tribol* **127**: 248–253 (2005)
- [17] Kovalchenko A, Ajayi O, Erdemir A, Fenske G, Etsion I. The effect of laser surface texturing on transitions in lubrication regimes during unidirectional sliding contact. *Tribol Int* **38**: 219–225 (2005)
- [18] Ryk G, Kligerman Y, Etsion I, Shinkarenko A. Experimental investigation of partial laser surface texturing for piston-ring friction reduction. *Tribol Trans* **48**: 583–588 (2005)
- [19] Ryk G, Etsion I. Testing piston rings with partial laser surface texturing for friction reduction. *Wear* **261**: 792–796 (2006)
- [20] Lu P, Wood R J K. Tribological performance of surface texturing in mechanical applications-A review. *Surf Topogr Metrol Prop* **8**: 043301 (2020)
- [21] Braun D, Greiner C, Schneider J, Gumbsch P. Efficiency of laser surface texturing in the reduction of friction under mixed lubrication. *Tribol Int* **77**: 142–147 (2014)
- [22] Costa H L, Hutchings I M. Hydrodynamic lubrication of textured steel surfaces under reciprocating sliding conditions. *Tribol Int* **40**: 1227–1238 (2007)
- [23] Arslan A, Masjuki H H, Kalam M A, Varman M, Mosarof M H, Mufti R A, Quazi L M M, Khuong S, Liaqat M, Jamshaid M, et al. Investigation of laser texture density and diameter on the tribological behavior of hydrogenated DLC coating with line contact configuration. *Surf Coatings Technol* **322**: 31–37 (2017)
- [24] Sedlaček M, Podgornik B, Ramalho A, Česnik D. Influence of geometry and the sequence of surface texturing process on tribological properties. *Tribol Int* **115**: 268–273 (2017)
- [25] Tomanik E. Friction and wear bench tests of different engine liner surface finishes. *Tribol Int* **41**: 1032–1038 (2008)
- [26] Mezghani S, Demirci I, Zahouani H, El Mansori M. The effect of groove texture patterns on piston-ring pack friction. *Precis Eng* **36**: 210–217 (2012)
- [27] Grabon W, Pawlus P, Wos S, Koszela W, Wieczorowski M. Effects of cylinder liner surface topography on friction and wear of liner-ring system at low temperature. *Tribol Int* **121**: 148–160 (2018)
- [28] Rao X, Sheng C, Guo Z, Yuan C. Influence of surface groove width on tribological performance for cylinder liner-piston ring components. *Tribol Trans* **62**: 239–248 (2019)
- [29] Grabon W, Pawlus P, Wos S, Koszela W, Wieczorowski M. Effects of honed cylinder liner surface texture on tribological properties of piston ring-liner assembly in short time tests. *Tribol Int* **113**: 137–148 (2017)
- [30] Rao X, Sheng C, Guo Z, Zhang X, Yin H, Xu C, Yuan C Q. Effects of textured cylinder liner piston ring on performances of diesel engine under hot engine tests. *Renew Sustain Energy Rev* **146**: 111193 (2021)
- [31] Miao C W, Guo Z W, Yuan C Q. Tribological behavior of co-textured cylinder liner-piston ring during running-in. *Friction* **10**(6): 878–890 (2022)
- [32] Pettersson U, Jacobson S. Influence of surface texture on boundary lubricated sliding contacts. *Tribol Int* **36**: 857–864 (2003)
- [33] Al-Azizi A A, Eryilmaz O, Erdemir A, Kim S H. Nano-texture for a wear-resistant and near-frictionless diamond-like carbon. *Carbon* **73**: 403–412 (2014)
- [34] He D, Zheng S, Pu J, Zhang G, Hu L. Improving tribological properties of titanium alloys by combining laser surface texturing and diamond-like carbon film. *Tribol Int* **82**: 20–27 (2015)



- [35] Zavedeev E V, Zilova O S, Barinov A D, Shupegin M L, Arutyunyan N R, Jaeggi B, Neuenschwander B, Pimenov S M . Femtosecond laser microstructuring of diamond-like nanocomposite films. *Diam Relat Mater* **74**: 45–52 (2017)
- [36] Araujo J A, Souza R M, De Lima N B, Tschiptschin A P. Thick CrN/NbN multilayer coating deposited by cathodic arc technique. *Mater Res* **20**: 200–209 (2017)
- [37] Ferreira R, Carvalho, Pires J, Sobral L, Carvalho S, Silva F. A new tribometer for the automotive industry: development and experimental validation. *Exp Mech* **62**: 483–492 (2022)
- [38] Gachot C, Rosenkranz A, Hsu S M, Costa H L. A critical assessment of surface texturing for friction and wear improvement. *Wear* **372–373**: 21–41 (2017)
- [39] Zavos A B, Nikolakopoulos P G. Simulation of piston ring tribology with surface texturing for internal combustion engines. *Lubr Sci* **27**: 151–176 (2015)
- [40] Schubert A, Neugebauer R, Sylla D, Avila M, Hackert M. Manufacturing of surface microstructures for improved tribological efficiency of powertrain components and forming tools. *CIRP J Manuf Sci Technol* **4**: 200–207 (2011)
- [41] Wos S, Koszela W, Pawlus P. Determination of oil demand for textured surfaces under conformal contact conditions. *Tribol Int* **93**: 602–613 (2016)



**Rita FERREIRA.** She received her M.Sc. degree in mechanical engineering in 2014 from University of Minho, Portugal. She joined the Center for MicroElectroMechanical Systems in 2016, in the mechanical engineering group. After then she enrolled in an Massachusetts Institute of

Technology (MIT) Portugal Doctoral Program with a Ph.D. in industry, in cooperation with MAHLE, Componentes de Motores, S.A.. Now she is a Ph.D. candidate of leaders for technical industries at the University of Minho. Her research areas cover the tribology of mechanical parts, manufacturing, and composite materials development for functional surfaces.